

Constructing a better binding peptide for drug delivery targeting the interleukin-4 receptor

Xue-Di Bai^a, Xue-Wei Cao^a, Yi-Hui Chen^a, Long-Yun Fu^b, Jian Zhao^a and Fu-Jun Wang^{b,c}

^aState Key Laboratory of Bioreactor Engineering, East China University of Science and Technology, Shanghai, China; ^bZhejiang Fonow Medicine Co. Ltd., Dongyang, China; ^cInstitute of Chinese Materia Medica, Shanghai University of Traditional Chinese Medicine, Shanghai, China

ABSTRACT

Targeted delivery of antitumor drugs is especially important for tumour therapy. Tumour targeting peptides have been shown to be very effective drug carriers for tumour therapy. Interleukin-4 receptor (IL-4R) is overexpressed on the surface of various human solid tumours. To obtain a better targeting peptide, we first designed a novel targeting peptide derived from interleukin-4 (IL-4), ILBP-b. ILBP-b contains the key high-affinity binding residue E9 of IL-4 to IL-4R. Compared with a reported targeting peptide ILBP-a (containing another key high affinity residue R88), ILBP-b was proved to be a better targeting peptide by the fluorescence experiments. Then, we further fused ILBP-b and ILBP-a to increase the multisite-binding ability of ILBP-b and got a better targeting peptide ILBP-ba. ILBP-ba showed a stronger preferential binding ability to IL-4R high-expressing cells than ILBP-a and ILBP-b. Competitive binding experiments demonstrated ILBP-ba specifically targets IL-4R. By fusing ILBP-ba with drug protein trichosanthin (TCS), *in vitro* drug carrying experiments showed that ILBP-ba could specifically enhance the killing effect of TCS on IL-4R high-expressing tumour cells (more than 10 folds). These results indicated that ILBP-ba has great potential for drug delivery applications targeting IL-4R and will be beneficial for the development of tumour therapeutic agents.

ARTICLE HISTORY

Received 18 January 2020
Revised 6 April 2020
Accepted 27 April 2020

KEYWORDS

Tumour-targeting peptide; interleukin-4 receptor; drug delivery; interleukin-4; trichosanthin (TCS)

Introduction

Although the first-line antitumor drugs commonly used in clinical practice have good therapeutic effects, these drugs usually cause severe toxicity and side effects in normal human cells during tumour treatment [1]. Targeted drug therapy methods that specifically deliver therapeutic drugs to tumour cells by targeting high-expressing receptors on tumour cells are preferable because of their better efficacy and safety [2–4]. A number of effective targeted therapies have been introduced, such as those that utilise receptors that are highly expressed on tumour cell surfaces. These receptors include epidermal growth factor receptor (EGFR) [2], human epidermal growth factor receptor-2 (HER2) [3] and vascular endothelial growth factor receptor (VEGFR) [4]. However, due to the diversity of different tumour cells, these receptors are not always highly expressed or have been mutated in some tumour cells. For example, EGFRs are only overexpressed in 50–70% of lung cancers, colon cancer and breast cancer [5]. Moreover, mutant EGFR is a promising target for non-small-cell lung cancer, such as the L858R mutation [6–8]. However, this kind of EGFR is only present in 20% of lung cancer patients [6]. In addition, due to the selective pressure that the drug places on cell survival, the use of a single type of targeted drug for an extended period of time may lead to drug resistance in the remaining tumour cells [6], resulting in compensatory upregulation of other signalling pathways (such as mesenchymal–epithelial conversion factor amplification or the EGFR T790M mutation) [9,10]. Therefore, the

application of more new drugs targeting different receptors in the clinic may result in better long-term therapeutic effects for patients.

Many types of tumour cells, including lung cancer cells, cervical cancer cells and breast cancer cells, typically overexpress interleukin-4 receptor (IL-4R) [6,11,12], while normal cells (including immune cells) express notably low levels of IL-4Rs [13]. There are three types of IL-4R present on the surfaces of human cells. Among these types, type I consists of the IL-4R α and IL-2R γ c chains; type II consists of the IL-4R α and IL-13R α 1 chains, which is overexpressed in solid tumours; and type III is composed of the IL-4R α , IL-2R γ c and IL-13R α 1 chains (Figure 1(A)) [14]. After the ligand binds to IL-4R, the complex will be efficiently internalised into the cells [11]. This potentially useful binding property can be used to deliver chemotherapeutic drugs, proteins and siRNAs to tumour cells via IL-4R-mediated endocytosis [15]. In addition, the interaction between interleukin-4 (IL-4, one of the IL-4R ligands) and IL-4R in humans promotes tumour cell proliferation and metastatic growth through a variety of signalling pathways [16]. The interaction of IL-4 with IL-4R also affects many signalling pathways that induce the expression of several anti-apoptotic proteins, such as Bcl-xL, Bcl-2 and cFLIP. These antiapoptotic proteins contribute to tumour cell survival and their resistance to drug-induced apoptosis [17–19]. Thus, the therapeutic efficacy of anticancer drugs can be enhanced by reducing the interaction between IL-4 and IL-4R [12,17,20]. For example, when anti-IL-4 antibodies were used to prevent IL-4 from binding to IL-4R, the resistance of tumour cells

CONTACT Jian Zhao  zhaojian@ecust.edu.cn  State Key Laboratory of Bioreactor Engineering, East China University of Science and Technology, 130 Meilong Road, Shanghai 200237, China; Fu-Jun Wang  wfj@shutcm.edu.cn  Institute of Chinese Materia Medica, Shanghai University of Traditional Chinese Medicine, 1200 Cailun Road, Shanghai 201203, China

 Supplemental data for this article can be accessed [here](#).

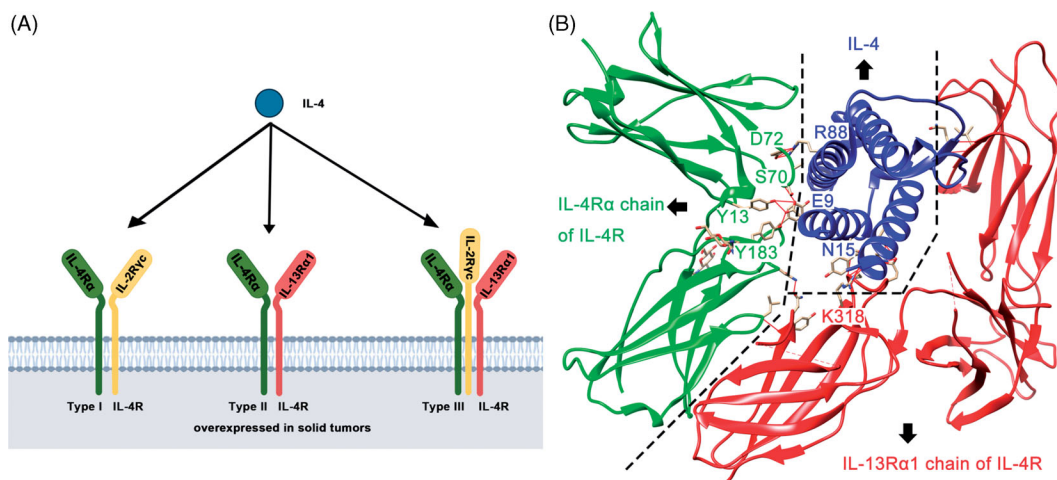


Figure 1. Schematic diagram of three types of IL-4R and hydrogen bond analysis of key binding sites of human IL-4 and type II IL-4R. (A) A schematic diagram of three types of IL-4R. Type II IL-4R is overexpressed in many solid tumours (B) Hydrogen bond binding analysis map of key binding sites of human IL-4 and type II IL-4R. Information about the structure comes from the Protein Data Bank and the simulation map was displayed using the UCSF Chimera software (RBVI).

to drugs was strongly reduced [20]. In addition, several studies have shown that IL-4R is an effective target for the clinical treatment of different tumours [21–26]. Therefore, IL-4R, as one of the overexpressed markers on tumour cells, is considered a suitable molecular target for tumour-targeted therapy, which can be used to enrich the types of therapeutic targets and to improve the deficiencies of conventional targets in tumour-targeted therapies.

As a natural ligand for IL-4R, human interleukin-4 (hIL-4) first interacts strongly with IL-4R α chain through two key residues E9 and R88 of hIL-4, which contribute the greatest affinity in the interaction between hIL-4 and IL-4R. Subsequently, the complex formed by hIL-4 and IL-4R α recruits IL-13R α 1 chain with low affinity via the key residues I11, N15, R121 and Y124 of hIL-4 (Figure 1(B)) [14]. Finally, the final complex will be internalised into the cell. Researchers have utilised this specific binding property of hIL-4 and type II IL-4R for tumour-targeted drug therapy. For example, a fusion protein of hIL-4 and *Pseudomonas* exotoxin A (hIL-4-PE) showed good targeting capacity to biliary cancer cells overexpressing IL-4R [27]. However, full-length hIL-4 is a multifunctional pleiotropic cytokine that regulates many immune responses, including T helper 2 cell differentiation, parasitic clearance, mucus secretion and eosinophil activation [28]. Moreover, as mentioned above, full-length hIL-4 can promote the proliferation, metastatic growth and drug resistance of tumour cells. Therefore, full-length hIL-4 is not suitable to be used as a targeted delivery vector due to its numerous biological functions. Rational selection of the binding domain of hIL-4 as a specific IL-4R-binding peptide (ILBP) is a common strategy for solving such problems [29]. For example, a short peptide of hIL-4 containing the key residue R88, KQLIRFLKRLDR₈₈N (abbreviated in this report as IL-4R-binding peptide a, ILBP-a), was selected to form a hybrid peptide IL-4R α -lytic [26]. Compared with the lytic peptide alone, IL-4R α -lytic significantly decreased the 50% inhibition concentration (IC₅₀) values of the lytic peptide against multiple IL-4R high-expressing tumour cells (2.8- to 5.1-fold), while the decrease of IC₅₀ value in normal cell was weaker (2-fold). This experimental result demonstrated that a partial binding domain of IL-4 could be a good targeted delivery vector due to its good selectivity between tumour cells and normal cells. However, the inhibitory effect of lytic peptide was increased two fold in normal cell in which IL-4R was not detected. Furthermore, the fold decreased by ILBP-a in tumour

cells was not notably higher than that in normal cells. These findings indicated that ILBP-a has an opportunity for further optimisation. Therefore, it is possible to select a new binding domain of IL-4 or optimally engineer ILBP-a to obtain a better ILBP with a stronger binding capacity and a better targeting capacity to IL-4R for tumour-targeted drug delivery.

In this study, we analysed the molecular mechanisms of interaction between IL-4 and IL-4R, and found that another key high-affinity binding residue E9 has not been studied. Residue E9 has a similar high affinity for the IL-4R as residue R88 in ILBP-a. Therefore, we attempted to design a peptide containing E9 residue as a novel targeting peptide to target IL-4R. A short peptide derived from helix A (HKCDITLQE₉I₁₁KTLN₁₅SLT, named ILBP-b) was selected as an ILBP, and its selectivity for IL-4R was characterised in IL-4R high-expressing cells (H226, A459 and HeLa) and IL-4R low-expressing cells (SMMC). Subsequently, in order to further enhance the targeting ability of ILBP-b, we recombined ILBP-a and ILBP-b in different order and obtained a more optimised targeting peptide ILBP-ba which has multi-site binding ability (containing E9 and R88) to IL-4R. The properties of ILBP-ba were fully characterised, including comparative analysis of targeted binding capacity between different cells, target analysis with different ligand competitions, analysis of drug transport and so on. Through the above experiments, we got a more powerful and specific targeting peptide that can deliver antitumor drugs to cells via IL-4R.

Materials and methods

Reagents and antibodies

The plasmid extraction kit, the PCR product purification kit, and the gel recovery kit were all purchased from Genesay Biotech Company (Shanghai, China). 4',6-Diamidino-2-phenylindole (DAPI), 4% paraformaldehyde (PFA), kanamycin, isopropyl- β -D-1-thiogalactopyranoside (IPTG) and 3-(4,5-dimethylthiazol-2-yl)-2,5-diphenyl tetrazolium bromide (MTT) were obtained from Beyotime Institute of Biotechnology (Shanghai, China). The BCA protein assay kit was purchased from Guangzhou Dingguo Biotechnology Co. Ltd. (Guangzhou, China). The Annexin V-FITC apoptosis detection kit was obtained from SONY (Shanghai, China). DNA polymerase, restriction enzymes and T4 DNA ligase were purchased from the

Takara Company (Dalian, China). *Escherichia coli* BL21 (DE3) cells were obtained from ComWin Biotech Company (Beijing, China). Polyclonal antibodies against IL-4R α and GAPDH and horseradish peroxidase-conjugated antibodies were obtained from Affinity (Shanghai, China). Nickel-nitrilotriacetic acid (Ni-NTA) agarose resin was maintained in our laboratory. Full-length IL-4 was purchased from Shenggong (Shanghai, China).

Construction of plasmids

Plasmids EGFP pET28a and TCS pET28b were maintained in our laboratory. Plasmids EGFP-ILBP-a pET28a and EGFP-ILBP-b pET28a were each synthesised by Generey Corporation (Generey, Shanghai, China). Then, ILBP-a and ILBP-b were amplified from EGFP-ILBP-a pET28a and EGFP-ILBP-b pET28a by polymerase chain reaction and cloned into EGFP-ILBP-a pET28a by *Hind* III and *Xho* I to obtain the EGFP-ILBP-aa pET28a, EGFP-ILBP-bb pET28a, EGFP-ILBP-ab pET28a and EGFP-ILBP-ba pET28a plasmids (Figure S1A). The plasmids TCS-ILBP-a pET28b and TCS-ILBP-ba pET28b were constructed based on TCS pET28b by cloning ILBP-a and ILBP-ba using *Eco*R I and *Xho* I (Figure S1A).

Preparation of proteins

Each recombinant plasmid was transformed into *Escherichia coli* BL21 (DE3) cells. Then, the BL21 cells were cultured in 30 ml of fresh LB medium with 50 μ g/ml kanamycin for 12 h at 37 °C. Subsequently, 4 ml of bacterial liquid was added into 200 ml of LB medium containing 50 μ g/ml kanamycin and grown for 2–3 h at 37 °C until the OD₆₀₀ reached 0.6–0.8 as measured by a UV-5200 Spectrophotometer (Yuan Xi, Shanghai, China). The bacterial cells were induced by 0.5 mM IPTG at 16 °C. After 16 h, all bacterial cells were harvested by centrifuging at 3500 \times g for 20 min at room temperature in a DL-5-B large-capacity low-speed centrifuge (Anke, Shanghai, China), and the medium was discarded. The cells were resuspended in buffer (20 mM Tris-HCl, 0.5 M NaCl, 5% glycerol, pH 8.5) and were sonicated to release the fusion proteins. After centrifuging at 12,000 \times g for 15 min, the supernatant of each recombinant protein was purified by Ni-NTA affinity chromatography according to the standard protocol. Protein concentration was determined by a BCA kit, and protein purity was determined by SDS-PAGE (Figure S1B). The protein was stored at -80 °C for subsequent experimental research.

Cell lines and cell culture conditions

The human non-small-cell lung tumour cell line NCI-H226 (abbreviated as H226) and A549, human cervical tumour HeLa, and human liver tumour SMMC-7721 (referred to as SMMC) cell lines were cultured in RPMI-1640 medium (HyClone, Logan, UT) supplemented with 10% foetal bovine serum (HyClone, Logan, UT), streptomycin (100 U/ml) and penicillin (100 μ g/ml). All cells were incubated at 37 °C in a 5% CO₂ atmosphere. All cells were laboratory-preserved.

Western blot analysis

H226, A549, HeLa and SMMC cells were cultured in 55-cm² culture dishes (Costar, Sacramento, CA). The digested cells were collected through centrifugation at 1000 \times g for 6 min at 4 °C in a high-speed freezing centrifuge and washed twice with PBS. Then, the cells were lysed with RIPA Lysis Buffer (Beyotime, Shanghai, China)

supplemented with protease inhibitor (MCE). The concentration of the supernatant protein was measured using the BCA protein assay kit according to the manufacturer's instructions. After treatment with SDS loading buffer, equal amounts of samples were separated by SDS-PAGE. The proteins in the gels were transferred to polyvinylidene fluoride membranes, and the membranes were then blocked in 5% non-fat milk for 6 h at room temperature, washed three times (10 min each) with PBS containing 0.1% Tween 20 (PBST20) and incubated with primary antibody specific for IL-4R α and GAPDH, dissolved in PBS containing 0.1% Tween and 1% non-fat milk powder at a 1:1000 dilution overnight at 4 °C. Subsequently, the membranes were washed three times with PBST20 and incubated with horseradish peroxidase-conjugated anti-rabbit secondary antibody for 1 h at room temperature. The expression levels of IL-4R were detected through autoradiography using a chemiluminescence imaging system (Tanon 5200, Shanghai, China).

Fluorescence microscopy

H226, A549, HeLa and SMMC cells were seeded in 48-well plates to approximately 60% confluence. After 12 h, the cells were treated with EGFP, EGFP-ILBP-a, EGFP-ILBP-b, EGFP-ILBP-aa, EGFP-ILBP-bb, EGFP-ILBP-ab and EGFP-ILBP-ba at different concentrations (5 μ M or 20 μ M). After incubation for 12 h at 37 °C, the cells were rinsed with precooled PBS (137 mM NaCl, 2.7 mM KCl, 10 mM Na₂HPO₄ and 2 mM KH₂PO₄) three times and fixed with 4% PFA for 30 min at 4 °C. Next, the cells were rinsed twice with PBS and stained with DAPI for 1 h. Finally, the samples were observed under a confocal laser scanning microscope (CLSM, Nikon, Tokyo, Japan).

Flow cytometry

H226 and SMMC cells were seeded in six-well plates to approximately 60% confluence. After 12 h, the cells were treated with EGFP, EGFP-ILBP-a, EGFP-ILBP-b, EGFP-ILBP-aa, EGFP-ILBP-bb, EGFP-ILBP-ab and EGFP-ILBP-ba at the concentration of 5 μ M. After treatment for 36 h, all cells were digested and collected. Then, the cells were harvested by centrifuging at 1000 \times g for 6 min at 4 °C in a high-speed freezing centrifuge (Xiang Yi, Shanghai, China) and washed twice with PBS. Subsequently, the treated samples (1 \times 10⁴ cells) were then analysed with a FACScan flow cytometer (Becton Dickinson, Franklin Lakes, NJ).

Competitive binding assay

A549 or HeLa cells (1.0 \times 10⁴/well) were seeded in 24-well plates (Costar, Sacramento, CA) to approximately 60% confluence in 1640 medium (HyClone, Logan, UT) supplemented with 10% foetal bovine serum (HyClone, Logan, UT). After 12 h of culture, the culture medium in control wells was replaced with fresh medium, and the culture medium in test wells was replaced with fresh medium and 10 μ M IL-4 or 10 ng/ml of anti-IL-4R antibody. After 1 h of culture at 4 °C, 5 μ M or 10 μ M EGFP-ILBP-a, EGFP-ILBP-b, EGFP-ILBP-aa, EGFP-ILBP-ab, EGFP-ILBP-ba and EGFP-ILBP-bb recombinant proteins were added to the control wells and test wells. After incubation for 2 h at 4 °C, the cells were rinsed with precooled PBS (137 mM NaCl, 2.7 mM KCl, 10 mM Na₂HPO₄ and 2 mM KH₂PO₄) three times and fixed with 4% PFA for 30 min at 4 °C. Next, the cells were rinsed twice with PBS and stained with

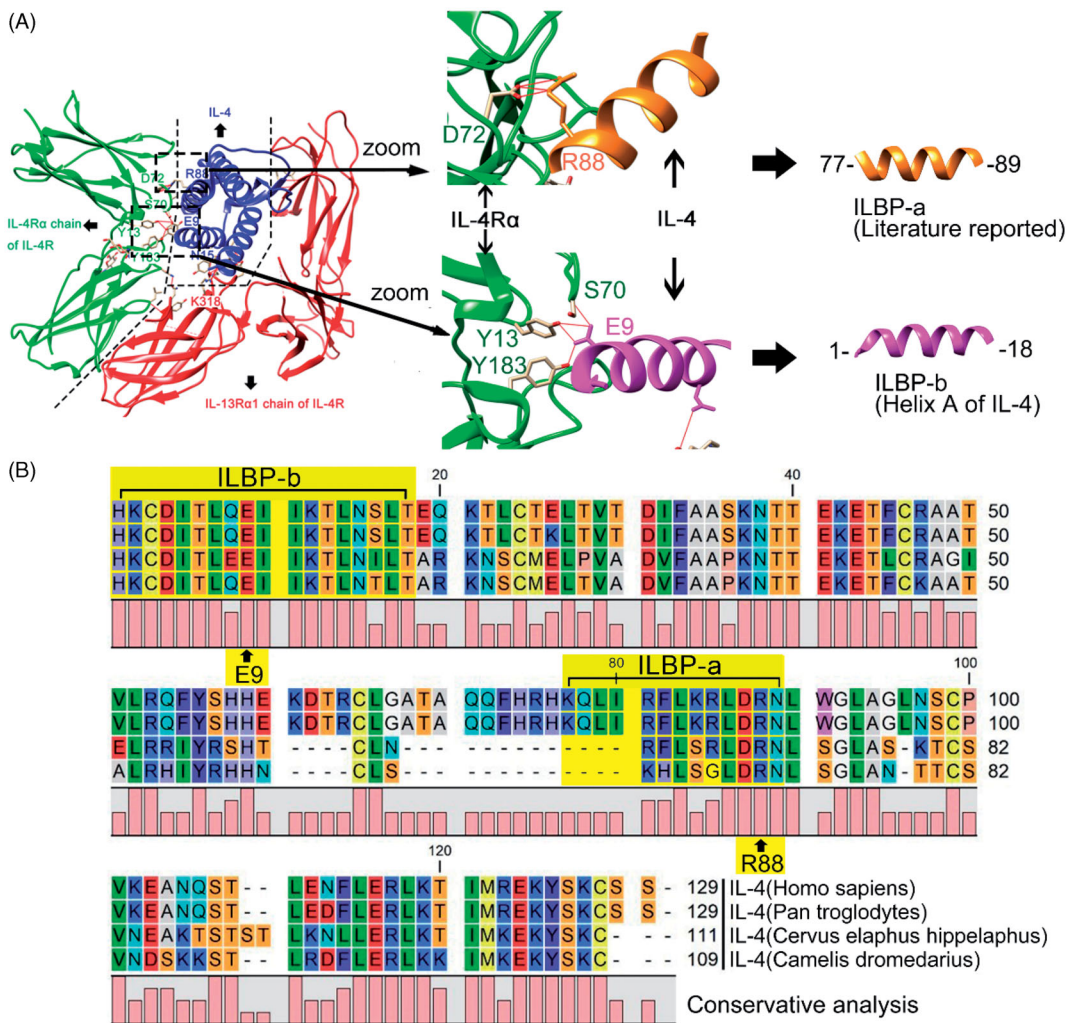


Figure 2. ILBP-b, the helix A of IL-4, was designed as a targeting peptide. (A) A simulation diagram of the contact interface structure of human IL-4 and IL-4R. Information about the structure comes from the Protein Data Bank and the simulation map is displayed using the UCSF Chimera software. (B) Sequence alignment of IL-4 from different species. The IL-4 sequences from different species were aligned using the CLC Main Workbench program. These four IL-4s were from *Homo sapiens*, *Pan troglodytes*, *Cervus elaphus hippelaphus* and *Camelus dromedarius*.

DAPI for 1 h. Finally, the samples were observed under a confocal laser scanning microscope (CLSM, Nikon, Tokyo, Japan).

In vitro targeted delivery simulation experiment

An *in vitro* simulation assay was designed to mimic the targeted delivery by ILBP-ba between IL-4R high-expressing cells and low-expressing cells *in vivo*. A coverslip was placed into each cell culture dish. Then, H226, A549, HeLa and SMMC cells were seeded in cell culture dishes. After incubation for 12 h, the coverslips containing each cell type were carefully transferred to the same cell culture dish filled with fresh medium. Subsequently, recombinant protein EGFP-ILBP-ba was added into the cell culture dish at the final concentration of 5 μ M. After incubation for 12 h, the fluorescence intensity in each cell was determined by microscopy (Nikon, Tokyo, Japan).

Cytotoxicity assay of ILBP-ba itself

The cytotoxicity of EGFP-ILBP-a and EGFP-ILBP-ba was assessed in HeLa cells with an MTT assay. Cells were cultured in 96-well plates (Costar, Sacramento, CA) to approximately 60% confluence. After 12 h of incubation, the cells were treated with EGFP, EGFP-ILBP-a and EGFP-ILBP-ba at different concentrations (0, 500 and 1000 nM) for

72 h. After incubation, 200 μ l of MTT mixed solution was added to each well, and the cells were incubated for 4 h. The supernatant was then removed, and 150 μ l DMSO was added to each well. The absorbance of each well was measured by a microplate reader at a wavelength of 492 nm.

Cell viability assay

The cytotoxicity of TCS, TCS-ILBP-a and TCS-ILBP-ba was also assessed in four cancer cell lines (H226, A549, HeLa and SMMC) with an MTT assay. Cells were cultured in 96-well plates (Costar, Sacramento, CA) to approximately 60% confluence. After 12 h of incubation, the cells were treated with TCS, TCS-ILBP-a and TCS-ILBP-ba at different concentrations (0, 200, 500, 800 and 1000 nM) for 72 h. After incubation, 200 μ l of MTT mixed solution was added to each well, and the cells were incubated for 4 h. The supernatant was then removed, and 150 μ l of DMSO was added to each well. The absorbance of each well was measured by a microplate reader at a wavelength of 492 nm.

Apoptosis analysis

Apoptosis was analysed using an Annexin V-FITC apoptosis detection kit. Briefly, H226 and SMMC cells were added to six-well

Table 1. Amino acid sequence of ILBPs.

Name	AA sequence ^a
ILBP-b	HKCDITLQEIHKTLNLSLT
ILBP-aa	KQLIRFLKRLDRNGGGGSKQLIRFLKRLDRN
ILBP-bb	HKCDITLQEIHKTLNLSLTGGGGSHKCDITLQEIHKTLNLSLT
ILBP-ab	KQLIRFLKRLDRNGGGGSHKCDITLQEIHKTLNLSLT
ILBP-ba	HKCDITLQEIHKTLNLSLTGGGGSKQLIRFLKRLDRN

^aLinker peptide residues are underlined.

plates (Costar, Sacramento, CA) to approximately 60% confluence (1.0×10^4 /well) and incubated for 12 h. TCS, TCS-ILBP-a and TCS-ILBP-ba were added at the final concentration of 500 nM. After treatment for 36 h, all cells were harvested by centrifuging at $1000 \times g$ for 6 min at 4 °C in a high-speed freezing centrifuge (Xiang Yi, Shanghai, China) and were washed twice with PBS. Subsequently, the cells were resuspended in 500 μ l of $1 \times$ Annexin V Binding Solution. Thereafter, 5 μ l of Annexin V-PE and 5 μ l of propidium iodide (PI) were added, and the cells were incubated at 20 °C for 20 min in the dark. Then, the treated samples (1×10^4 cells) were analysed with a FACScan flow cytometer (Becton Dickinson, Franklin Lakes, NJ) at an emission of 530 nm and an excitation of 488 nm.

Data and statistical analysis

Data were obtained from at least three independent experiments, and statistical analyses of data are shown as means \pm SDs. The grey value of the western blot strip was calculated by ImageJ. Student's *t*-test was performed using GraphPad Prism 7.0 (GraphPad Software, La Jolla, CA) to identify significance. $p < .05$ was considered to be statistically significant.

Results

Design of a novel IL-4R-binding peptide ILBP-b

IL-4R (type II) is overexpressed in many types of tumour cells [6,11,12]. During the binding of human IL-4 (hIL-4) to IL-4R, the residues E9 and R88 of hIL-4 play a key role due to their high affinity to the corresponding residues of IL-4R α chain (Y13, Y83 and S70, D72, Figure 2(A)) [14]. Yang et al. selected a short peptide (containing residue R88) of human IL-4 (77-KQLIRFLKRLDRN-89, named herein ILBP-a) as a targeting peptide [26]. However, it is not known why the peptide containing residue E9 was not designed as a targeting peptide. We believed that E9 can be designed as an important functional residue of the targeting peptide. Residue E9 is located in helix A of hIL-4 (1-HKCDITLQE₉IL₁₁KTLN₁₅SLT-18, named ILBP-b in this paper, Figure 2(A)). We analysed the hydrogen bond interaction between ILBP-b and IL-4R using UCSF Chimera (Figure 2(A)). The result showed that residue E9 of helix A forms three pairs of hydrogen bonds with IL-4R α (Y13, S70 and Y183). Moreover, sequence alignment analysis of IL-4 from different species by CLC Main Workbench software also showed that ILBP-b is a highly conserved sequence (Figure 2(B)), and ILBP-b is more conservative than ILBP-a. Therefore, we believed that ILBP-b of hIL-4 may have good binding capacity to IL-4R. The sequence of ILBP-b described above is shown in Table 1.

ILBP-b is a better IL-4R-targeting peptide than the reported targeting peptide ILBP-a

In order to select several cells for investigating the cell selectivity of ILBP-b, the IL-4R expression levels in H226, A549, HeLa and

SMMC cells were detected by western blot using an anti-IL-4R α antibody [30]. The western blot and semi-quantitative results are shown in Figure 3(A). All four cells showed significant expression of IL-4R, but their expression levels were different. Consistent with reports in the literature [6], H226 cells are cells with high IL-4R expression. Compared with H226, the IL-4Rs of A549 and HeLa cells were also highly expressed. However, the expression level of IL-4R in SMMC cells was much lower than that in the other three cells (approximately 2–4 folds lower). Thus, the above results indicated that H226, A549 and HeLa cells could be used as IL-4R high-expressing cells, and SMMC cells could be used as IL-4R low-expressing cells.

By fusion with a fluorescent 'tag', enhanced green fluorescent protein (EGFP) [31,32], we investigated whether ILBP-b highly targets IL-4R high-expressing cells by fluorescence binding experiments and flow quantification experiments. The reported targeting peptide ILBP-a was set as a control. As shown in Figure 3(B,C), EGFP did not show any fluorescence in all four cells, while the fusion proteins EGFP-ILBP-a and EGFP-ILBP-b showed obvious fluorescence to be observed in H226, A549, HeLa and SMMC cells at the concentration of 20 μ M. EGFP did not show any fluorescence, indicating that EGFP does not bind any cells. In H226, A549 and HeLa cells, EGFP-ILBP-b exhibited high-intensity fluorescence, similar to the control protein EGFP-ILBP-a. In SMMC cells, the fluorescence intensity of EGFP-ILBP-b was significantly lower than that in the other three cell lines and lower than that of EGFP-ILBP-a in SMMC cells (Figure 3(B)). Consistent with the fluorescence results, the difference of fluorescence intensity of EGFP-ILBP-b between the two cells was greater than that of EGFP-ILBP-a (Figure 3(C)). Moreover, the fluorescence intensities of EGFP-ILBP-a and EGFP-ILBP-b were consistent with the expression levels of IL-4R in the four cell lines. These results indicated that ILBP-b had better selectivity than ILBP-a to target IL-4R high-expressing cells.

Then, we investigated whether ILBP-b had specific binding capacities to IL-4R by a competitive binding assay in HeLa cells with 10 μ M IL-4 (Figure 3(D,E)). IL-4, a major ligand of IL-4R, might inhibit the binding of ILBP-b to cells because of competitive binding to IL-4R. At 4 °C, the metabolism of cell is slow, resulting in reduced endocytosis of IL-4R, which can eliminate the interference caused by IL-4R endocytosis [6]. Cells were first pre-incubated with excess IL-4 for 1 h at 4 °C to ensure that IL-4 can bind almost all IL-4R on the cell surface. If the target of ILBP-b is IL-4R, excessive IL-4 will hinder the binding of EGFP-ILBP-b, resulting in a greatly reduced fluorescence intensity of EGFP-ILBP-b. Two peptides HBP and ILBP-a were set as controls to investigate whether IL-4 specifically blocks IL-4R without blocking other targets. HBP, a peptide that the binding receptor was related to the heparan sulphate proteoglycan (HSPG) [33], dose not bind IL-4R. ILBP-a is a peptide specifically targeting IL-4R [26]. Since the fluorescence of EGFP-ILBP-a and EGFP-ILBP-b is too weak to be observed at low concentration (5 μ M), we replaced ILBP-a and ILBP-b with their tandem repeats (ILBP-aa and ILBP-bb) to enhance the affinity of the targeting peptides without changing their target (Figure 4(A), Table 1) [34]. As shown in Figure 3(D,E), after treated with IL-4, EGFP-HBP remains the same fluorescence intensity with the control group, and the fluorescence intensity of EGFP-ILBP-aa was significantly reduced (Figure 3(D)). Flow cytometry also showed that the fluorescence intensity of EGFP-ILBP-aa was reduced by about 70%, and the fluorescence intensity of EGFP-HBP remained unchanged (Figure 3(E)). These results indicated that IL-4 only hinders the binding of ILBP to cells. Thus, the fluorescence intensity of EGFP-ILBP-bb was significantly reduced after treated with IL-4

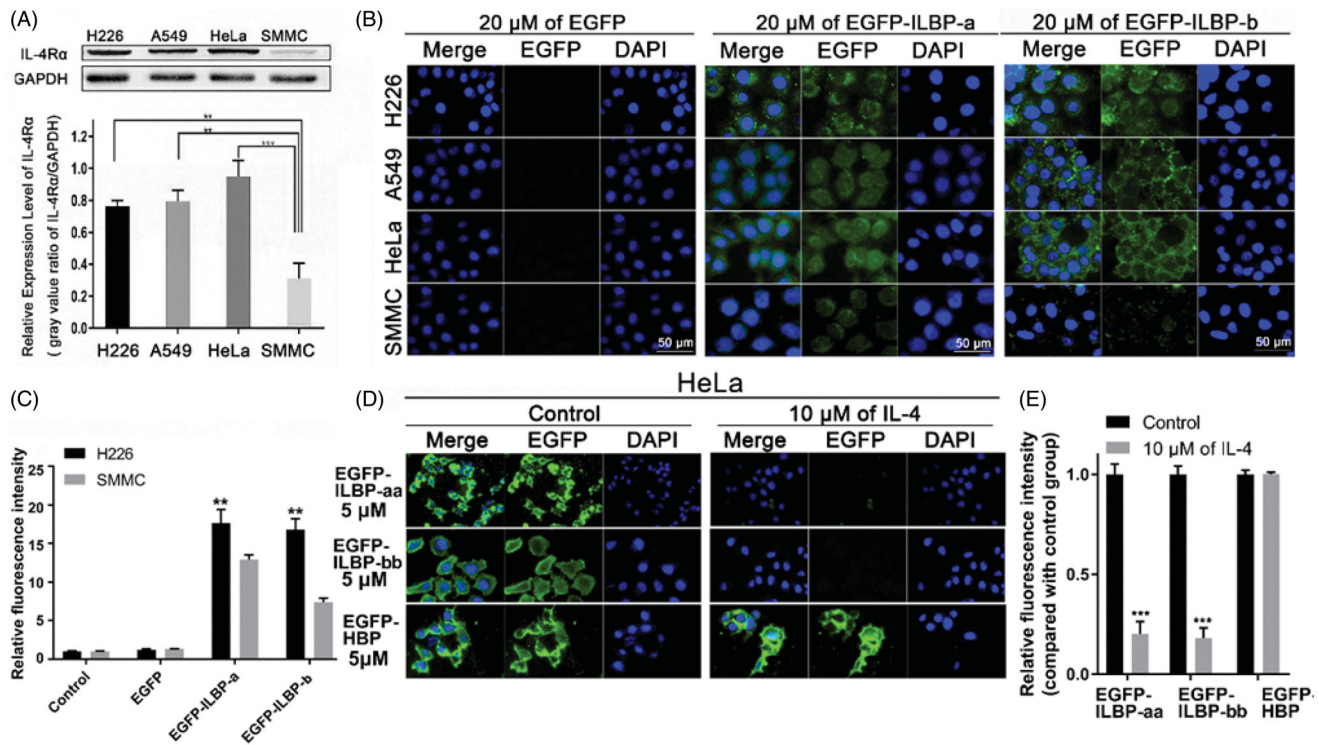


Figure 3. ILBP-b is a better IL-4R-targeted peptide than ILBP-a. (A) Expression of IL-4R α in different tumour cell lines. GAPDH was used as an internal control. Grey value analysis was performed on each lane in the Western blot results map using ImageJ software. The obtained values were used as the numerical results of IL-4R α relative expression levels in the manner of IL-4R α /GAPDH. The error bars represent the mean \pm SD, $N = 3$. ** $p < .01$, *** $p < .001$, compared with SMMC group. (B) The cell selectivity of ILBP-b was detected by fluorescence binding experiments, and better than the cell selectivity of ILBP-a. EGFP was a negative control and EGFP-ILBP-a was a positive control. H226, A549, HeLa, SMMC cells were incubated with 20 μ M EGFP, EGFP-ILBP-a and EGFP-ILBP-b for 12 h at 37 $^{\circ}$ C. Then, the cells were fixed with 4% PFA and stained with DAPI and visualised by fluorescence microscopy under the same optical setup conditions. (C) Flow quantitative results of EGFP-ILBP-a and EGFP-ILBP-b recombinant proteins. H226 and SMMC cells were treated with recombinant proteins at a concentration of 20 μ M for 12 h at 37 $^{\circ}$ C. The cellular binding of recombinant proteins was detected by fluorescence-activated cell sorting. The mean values of fluorescence intensity were calculated by Flowjo software. The error bars represent the mean \pm SD, $N = 3$. ** $p < .01$, compared with SMMC group. (D) Competitive binding assay treated with IL-4. 5 μ M of EGFP-ILBP-aa, EGFP-ILBP-bb and EGFP-HBP was added to pre-incubated HeLa cells with or without 10 μ M of IL-4 for 2 h at 4 $^{\circ}$ C. The group treated with EGFP-HBP was used as a control group. Then, the cells were fixed with 4% PFA and stained with DAPI and visualised by fluorescence microscopy under the same optical setup conditions. (E) Flow quantitative results of the fluorescence intensity of the control group and the group blocked with IL-4. The mean values of fluorescence intensity were calculated by Flowjo software and the relative fluorescence intensity was compared with the mean value of control group. The error bars represent the mean \pm SD, $N = 3$. *** $p < .001$, compared with control group.

(Figure 3(D,E)), indicating ILBP-b is an ILBP. These results indicated ILBP-b can specifically target IL-4R.

Based on the above results, ILBP-b is a targeting peptide that specifically targets IL-4R, and its targeting is stronger than ILBP-a.

Multisite-binding hybrid peptide ILBP-ba is a more optimised targeting peptide than ILBP-b

The fusion protein EGFP-ILBP-b showed extremely weak fluorescence in the H226, A549, HeLa and SMMC cells at low concentrations (5 μ M, Figure S2), indicating that ILBP-b only has weak affinities for IL-4R at low concentrations, resulting in limited targeting ability of ILBP-b. To obtain a better targeting peptide than ILBP-b, we recombined ILBP-a and ILBP-b in a different order to obtain two multisite-binding hybrid peptides, ILBP-ab and ILBP-ba (Figure 4(A), Table 1). Based on the result of ILBP-b, we hypothesised that the inclusion of more key binding residues in an ILBP may result in a stronger capacity to target IL-4R. Both ILBP-ab and ILBP-ba included two key high-affinity binding residues E9 and R88. Thus, ILBP-ab and ILBP-ba might have better cell selectivity than ILBP-b due to more key binding residues.

To investigate whether multisite-binding hybrid peptides ILBP-ab and ILBP-ba have better cell selectivity, we fused ILBP-ab and

ILBP-ba with EGFP, and performed fluorescence microscope observation experiments and flow quantification experiments.

Single-site repeating hybrid peptide ILBP-aa and ILBP-bb were served as controls. The results are shown in Figure 4(C-E). The fluorescence binding experiments and flow quantification experiments showed that EGFP-ILBP-a and EGFP-ILBP-b showed very weak fluorescence in the four cell lines at a concentration of 5 μ M (Figure 4(B,D)). At this same concentration, the fluorescence intensities of EGFP-ILBP-aa, EGFP-ILBP-bb, EGFP-ILBP-ab and EGFP-ILBP-ba fusion proteins were much higher than those of EGFP-ILBP-a and EGFP-ILBP-b (Figure 4(C,D)). Compared with EGFP-ILBP-aa, EGFP-ILBP-bb, EGFP-ILBP-ab and EGFP-ILBP-ba proteins, the difference of fluorescence intensity of EGFP-ILBP-ba between the IL-4R high-expressing cell group and the IL-4R low-expressing cell group was the largest (Figure 4(C,D)). Thus, the above results indicated that ILBP-ba had much better selective targeting ability and affinity than ILBP-a and ILBP-b. Therefore, ILBP-ba is a more optimised delivery vector than ILBP-b.

In order to further study whether ILBP-ba has the ability to transport targeted drugs *in vivo*, we designed a co-culture experiment to simulate the delivery *in vivo*. H226, A549, HeLa and SMMC cells were co-cultured in the same dish, and EGFP-ILBP-ba was added to the dish to observe whether ILBP-ba could preferentially target IL-4R high-expressing cell lines (Figure 4(E)). Consistent with the results in the well plates, ILBP-ba bound

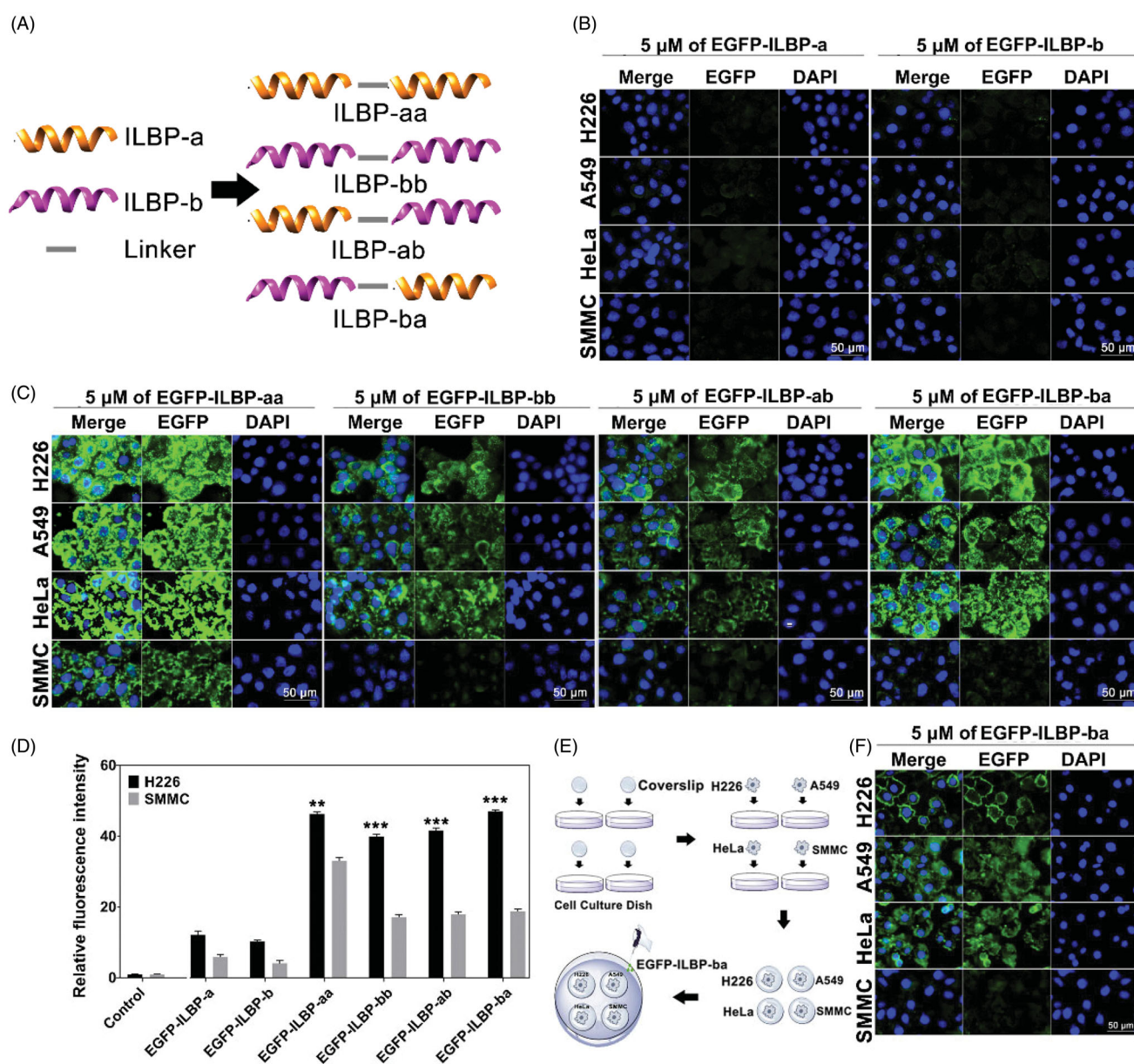


Figure 4. ILBP-ba is a more optimised targeting peptide than ILBP-b. (A) Schematic diagram of ILBP-aa, ILBP-bb, ILBP-ab and ILBP-ba. (B) The cellular selectivity of EGFP-ILBP-a and EGFP-ILBP-b at the concentration of 5 μM . H226, A549, HeLa and SMMC cells were incubated with 5 μM EGFP-ILBP-a and EGFP-ILBP-b for 12 h at 37 $^{\circ}\text{C}$. Then, the cells were fixed with 4% PFA and stained with DAPI and visualised by fluorescence microscopy under the same optical setup conditions. (C) The cellular selectivity of EGFP-ILBP-aa, EGFP-ILBP-bb, EGFP-ILBP-ab and EGFP-ILBP-ba at the concentration of 5 μM . The experimental methods were similar to (B). (D) Flow quantitative results of cellular selectivity of EGFP-ILBP-aa, EGFP-ILBP-bb, EGFP-ILBP-ab, EGFP-ILBP-ba recombinant proteins. H226 and SMMC cells were treated with recombinant proteins at a concentration of 5 μM for 12 h at 37 $^{\circ}\text{C}$. The cellular binding of recombinant proteins was detected by fluorescence-activated cell sorting. The mean values of fluorescence intensity were calculated by Flowjo software. The error bars represent the mean \pm SD, $N=3$. ** $p < .01$, *** $p < .001$, compared with SMMC group. (E) *In vitro* schematic diagram of cell-selective binding of ILBP-ba *in vivo*. Four cell lines were previously cultured on different coverslips, then transferred and placed in the same culture dish and incubated with 5 μM EGFP-ILBP-ba for 12 h at 37 $^{\circ}\text{C}$. (F) Cell-selective binding result of EGFP-ILBP-ba (5 μM) in schematic diagram. The experimental methods were similar to (B).

H226, A549 and HeLa cells with high affinity but only weakly bound SMMC cells (Figure 4(F)). This result further demonstrated that ILBP-ba had excellent targeted transportation capabilities for IL-4R-overexpressing cells.

Based on the above results, ILBP-ba is a more optimised targeting peptide than ILBP-b.

ILBP-ba specifically binds to IL-4R

We investigated whether ILBP-ba had the specific binding capacity to IL-4R by a competitive binding assay in A549 cells with 10 μM

IL-4 or 10 ng/ml anti-IL-4R α antibody. IL-4, one of the specific IL-4R ligands, might inhibit the binding of ILBP-ba to cells because of competitive binding to IL-4R. Also, the anti-IL-4R α antibody might inhibit the binding of ILBP-ba to IL-4R. The experimental principle and control setting were similar to the competitive binding assay of ILBP-b. ILBP-aa and HBP were also served as controls. The results of fluorescence experiments and flow quantification are shown in Figure 5. When A549 cells were pre-incubated with 10 μM IL-4, only the cells treated with EGFP-HBP still remained distinctly high fluorescence signals; other cells with the EGFP-ILBP-aa and EGFP-ILBP-ba group showed very weak fluorescence (70–75% inhibition, Figure 5(A,B)). When A549 cells were pre-incubated

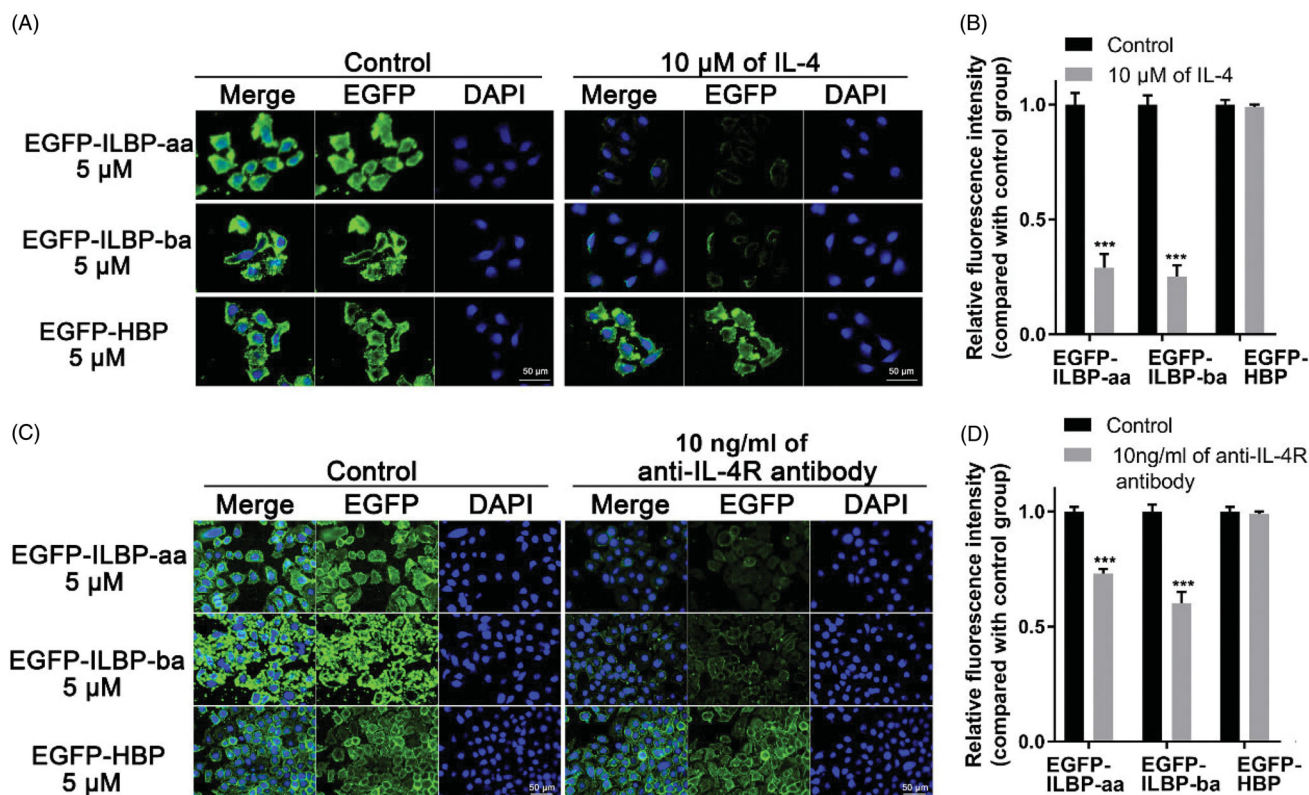


Figure 5. ILBP-ba specific binds to IL-4R. (A) Competitive binding assay treated with IL-4. 5 μM of EGFP-ILBP-aa, EGFP-ILBP-ba and EGFP-HBP were added to pre-incubated A549 cells with or without 10 μM of IL-4 for 2 h at 4 °C. The group treated with EGFP-HBP was used as a control group. Then, the cells were fixed with 4% PFA and stained with DAPI and visualised by fluorescence microscopy under the same optical setup conditions. (B) Flow quantitative results of the fluorescence intensity of the control group and the group blocked with IL-4. The mean values of fluorescence intensity were calculated by Flowjo software and the relative fluorescence intensity was compared with the mean value of control group. The error bars represent the mean \pm SD, $N = 3$. ** $p < .01$, *** $p < .001$, compared with control group. (C) Competitive binding assay treated with anti-IL-4R antibody. 5 μM of EGFP-ILBP-aa, EGFP-ILBP-ba, EGFP-ILBP-ab, EGFP-ILBP-ba and EGFP-HBP were added to pre-incubated A549 cells with or without 10 ng/ml of anti-IL-4R antibody for 2 h at 4 °C. (D) Flow quantitative analysis of the fluorescence intensity of the control group and the group blocked with anti-IL-4R antibody. The mean values of fluorescence intensity were calculated by Flowjo software and the relative fluorescence intensity was compared with the mean value of control group. The error bars represent the mean \pm SD, $N = 3$. *** $p < .001$, compared with control group.

with 10 ng/ml of anti-IL-4R antibody, the results were similar with result of the IL-4-treated group (Figure 5(C)). The inhibitory effect on EGFP-ILBP-aa and EGFP-ILBP-ba was 30–40% (Figure 5(D)). These results indicated that both IL-4 and anti-IL-4R antibody could specifically prevent the binding of ILBP-ba to tumour cells. Combining the results of the two sets of experiments, the fluorescence of EGFP-ILBP-ba was specifically inhibited, indicating that ILBP-ba could specifically bind to IL-4R.

ILBP-ba selectively enhances the cytotoxicity of drug to IL-4R high-expressing cells

Targeting peptides are generally non-toxic and safe [35]. In order to investigate whether ILBP-ba has such advantages, we assessed the cytotoxicity of ILBP-ba in HeLa cells. As a targeting peptide reported in literature, ILBP-a was also assessed as a control. The cytotoxicity of recombinant proteins EGFP, EGFP-ILBP-a and EGFP-ILBP-ba were examined by MTT assay. The result showed that the EGFP-ILBP-a and EGFP-ILBP-ba proteins did not show any cytotoxicity on HeLa cells (Figure 6(A)), and the 50% inhibitory concentration (IC_{50}) values of EGFP-ILBP-a and EGFP-ILBP-ba were very big and similar with that of EGFP (Table 2). This result showed that ILBP-ba do not have killing effect to cells within 1 μM, indicating that ILBP-ba is safe and non-toxic.

Trichosanthin (TCS) is a ribosome-inactivating protein that has antitumor activity against tumour cells [36]. To investigate whether ILBP-ba could selectively enhance the cytotoxicity of TCS

to IL-4R high-expressing cells, the cytotoxicity of TCS, TCS-ILBP-a and TCS-ILBP-ba recombinant proteins was examined by MTT assay in H226, A549, HeLa and SMMC cells. As shown in Figure 6(B), the killing effect of TCS-ILBP-ba on H226, A549 and HeLa cells was significantly improved than that of TCS and TCS-ILBP-a. For example, at a concentration of 500 nM, the killing effect of TCS-ILBP-ba was about 80%, while the killing effects of TCS and TCS-ILBP-a were less than 60%. The IC_{50} value of TCS-ILBP-ba was 10.71–13.99 folds lower than that of TCS, and 5.27–5.63 folds lower than that of TCS-ILBP-a. Moreover, the inhibition was positively correlated with the expression levels of IL-4R. In contrast, the killing effect of TCS-ILBP-ba on SMMC cells was not improved at any concentration. The IC_{50} value of the TCS-ILBP-ba fusion protein was almost the same as that of TCS and TCS-ILBP-a. Thus, the result indicated that ILBP-ba could selectively enhance the cytotoxic efficacy of TCS on IL-4R high-expressing cells, and the enhancement caused by ILBP-ba is stronger than that caused by ILBP-a.

The cytotoxic effect of TCS on cells was reported to be caused by inducing apoptosis [36]. To elucidate the mechanism of ILBP-ba selectively enhancing the cytotoxicity of TCS, the apoptotic effect induced by TCS-ILBP-ba was analysed in both H226 and SMMC cells by Annexin V-FITC/FACS analysis. The recombinant proteins TCS and TCS-ILBP-a were served as controls (Figure 6(C)). In H226 cells, compared with apoptotic rate caused by TCS alone (17.64%) and TCS-ILBP-a (26.9%), ILBP-ba could significantly increase the TCS-induced apoptotic rate of H226 cells (57.4%). In

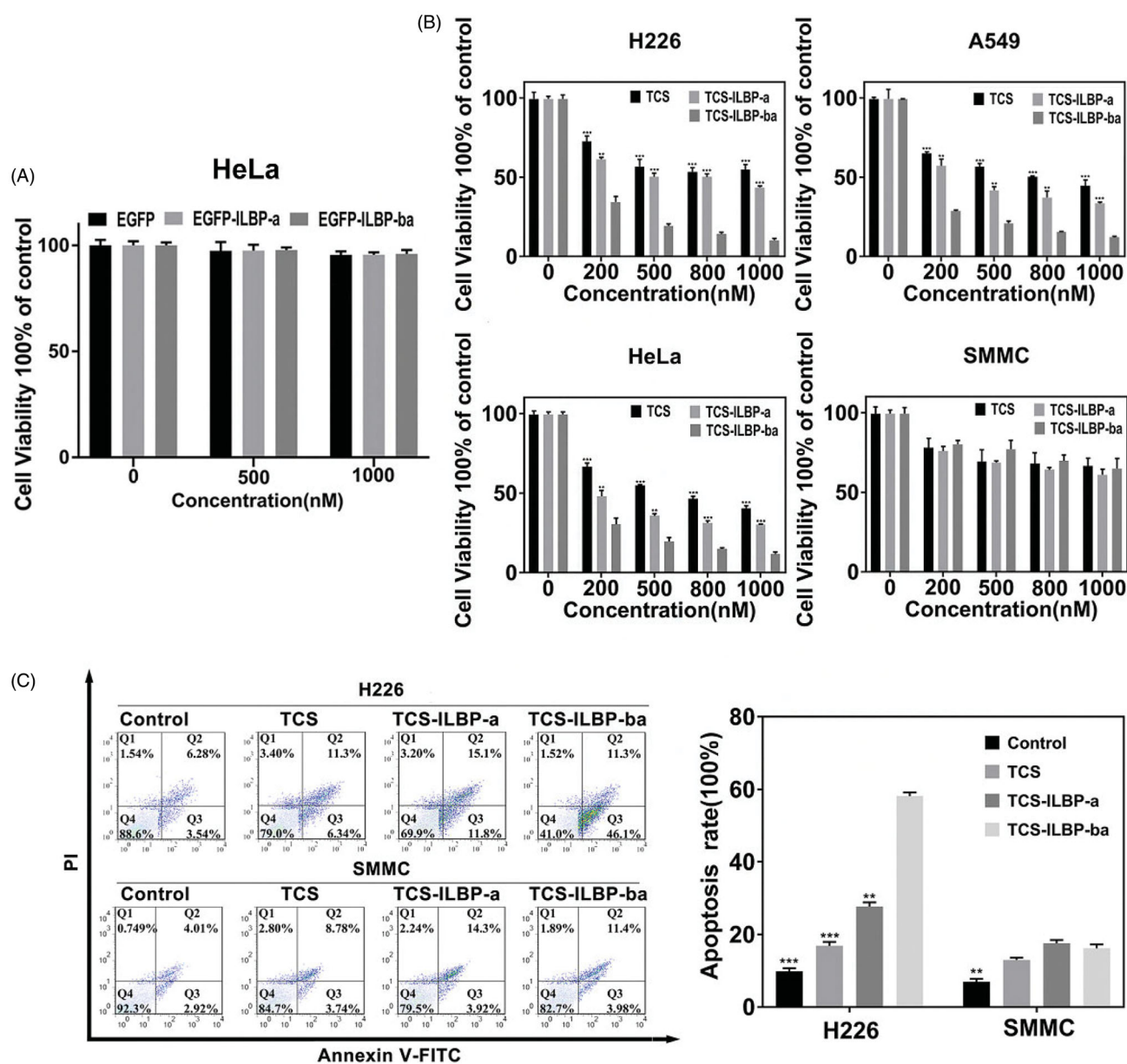


Figure 6. ILBP-ba selectively enhances the cytotoxicity of drug to IL-4R high-expressed cells. (A) *In vitro* cytotoxicity assay of ILBP-ba. HeLa cells were incubated with different concentrations of EGFP, EGFP-ILBP-a and EGFP-ILBP-ba proteins for 72 h at 37 °C. The inhibition ratio of EGFP, EGFP-ILBP-a and EGFP-ILBP-ba proteins on HeLa was measured by the MTT assay. The error bars represent the mean ± SD, N = 3. (B) Inhibition effects of different TCS-fused recombinant proteins on different cells. H226, A549, HeLa and SMMC cells were incubated with different concentrations of TCS, TCS-ILBP-a and TCS-ILBP-ba proteins for 72 h at 37 °C. The inhibition ratio of TCS, TCS-ILBP-a and TCS-ILBP-ba proteins on different cells was measured by the MTT assay. The error bars represent the mean ± SD, N = 3. ***p* < .01, ****p* < .001, compared with TCS-ILBP-ba group at each concentration. (C) Study of the cell death mechanism of the TCS series of recombinant proteins. H226 and SMMC cells were treated with 250 nM TCS, TCS-ILBP-a and TCS-ILBP-ba for 36 h, respectively. These cells were then collected and analysed using flow cytometry after being treated with Annexin V-FITC and propidium iodide. The experiment was performed three times. The histogram format of the apoptotic rate was shown in (C). The error bars represent the mean ± SD, N = 3. ***p* < .01, ****p* < .001, compared with TCS-ILBP-ba group.

Table 2. IC₅₀ values of different EGFP fusion proteins on HeLa.

Cells	IC ₅₀ (μM)		
	EGFP	EGFP-ILBP-a	EGFP-ILBP-ba
HeLa	39.23 ± 1.5	37.79 ± 1.2	36.18 ± 1.3

SMMC cells, TCS-ILBP-ba did not significantly altered TCS-induced apoptosis (15.38%) compared to that of TCS (12.52%) and TCS-ILBP-a (18.22%). These results clearly indicated that ILBP-ba could increase the ability of TCS to induce apoptosis in IL-4R high-expressing cells, so that ILBP-ba could selectively enhance the cytotoxicity of drug to IL-4R high-expressing cells.

Based on the above results, ILBP-ba could selectively enhance the cytotoxicity of drug to IL-4R high-expressing cells because ILBP-ba could increase the ability of TCS to induce apoptosis in IL-4R high-expressing cells. ILBP-ba is a better targeting peptide than ILBP-a.

Discussion

Traditional antitumor drugs commonly used in clinical practice often have serious toxic and side effects on normal cells [1]. The emergence of targeted therapies has dramatically reduced the side effects of these drugs [2–4]. As mentioned in section

Table 3. IC₅₀ values of different TCS fusion proteins on different tumour cell lines.

Cells	IC ₅₀ (nM)/decreased fold ^a		
	TCS	TCS-ILBP-a	TCS-ILBP-ba
H226	1208 ± 56	634.6 ± 45/1.90	112.7 ± 12/10.71
A549	771.5 ± 43	322.2 ± 34/2.39	61.07 ± 6/12.63
HeLa	888.6 ± 35	341.4 ± 25/2.60	63.47 ± 7/13.99
SMMC	4270 ± 260	3457 ± 221/1.24	3566 ± 183/1.20

^aValues compared to TCS.

'Introduction', a number of targeted therapies that utilise common receptors (such as EGFR) have some limitations [5–10]. Using IL-4R as a target could effectively enrich the therapeutic sites for targeted-drug therapies and reduce the limitations of common receptors in different cells [6,11–13,20]. In this study, we selected IL-4R as the target and designed a new binding peptide, ILBP-ba, with better binding capacity. ILBP-ba has high selectivity and affinity for IL-4R high-expressing cells according to the results of the fluorescence experiment (Figure 4) and the competitive binding experiment (Figure 5). Our MTT assay showed that ILBP-ba significantly improved the toxicity of TCS to H226, A549 and HeLa cells (10.71, 12.63 and 13.99 folds, respectively), but there was no significant cytotoxicity improvement in SMMC cells (1.2-fold). This TCS toxicity improvement by ILBP-ba was positively correlated with IL-4R expression levels of four cells (Figure 6(B), Table 3). In addition, the apoptosis experiment showed that ILBP-ba only significantly enhanced the TCS-induced apoptosis in H226 cells, but not in SMMC cells (Figure 6(C)), consistent with the expression levels of IL-4R on both cell surfaces. Through the experiments above, we demonstrated that ILBP-ba is a high-selectivity and high-affinity targeted transport vector for IL-4R and is suitable for tumour-targeting therapy.

Previous studies showed that the specific binding site of IL-4 could be used for targeted drug delivery [26]. A short peptide (K₇₇QLIR₈₁FLK₈₄R₈₅LDR₈₈N, ILBP-a) that harbours the high-affinity key binding residue R88 was chosen from hIL-4 to target IL-4R [26]. As mentioned in section 'Introduction', ILBP-a improved the inhibitory effect of the lytic peptide in both tumour cells (2.8–5.1 folds) and normal cells (two fold), but the fold difference between these two types of cells was not large enough. The reason for this might be that ILBP-a only binds to the IL-4R α chain. Three types of IL-4R are expressed on each cell and only type II IL-4R is over-expressed in many solid tumours. Since the IL-4R α chain is present in all three types, we speculated that ILBP-a might bind to three types of IL-4R without preference, resulting in the insufficient selectivity (Figure 7). Therefore, there is a need to obtain a better binding domain with stronger binding capacity and selectivity to IL-4R for targeted-drug delivery *in vivo*. After carefully examining the structure of IL4, we found that another high-affinity key binding residue E9 and other low-affinity key binding residues in IL-4 might be used for the construction of new targeting peptides. ILBP-b (H₁K₂CDITLQ₉II₁₁K₁₂TLN₁₅SLT) of IL-4 was selected to construct a new ILBP. The results in Figure 3 showed that ILBP-b has better cell selectivity than ILBP-a. We speculated on the cause of this result. Figure 7 shows both type II and type III IL-4R were involved with IL-4R α and IL-13R α 1 chain, which could be bound by the residues E9, I11 and N15 of ILBP-b. Therefore, ILBP-b was speculated to preferentially bind to type II or type III IL-4R. Due to the high expression of type II IL-4R in tumour cells, the specificity of ILBP-b is superior to ILBP-a.

However, the affinity of ILBP-b did not meet our expectations (Figure S3). Considering that more binding residues might result in more potent affinity and specific selectivity, four new binding

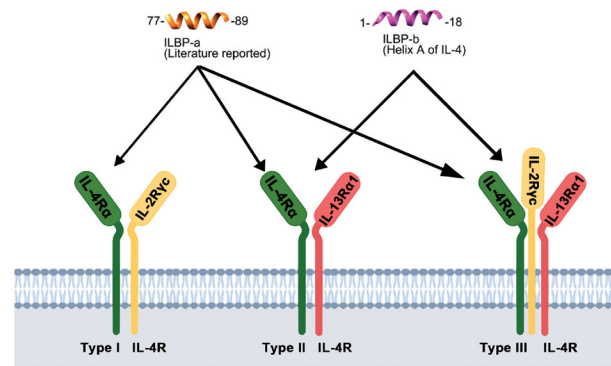


Figure 7. ILBP-b might preferentially target the type II or type III IL-4R. Schematic representation of the binding of ILBP-a and ILBP-b to three types IL-4R. ILBP-a could bind all three types of IL-4R. ILBP-b might more preferentially target the IL-4R composed of IL-4R α and IL-13R α 1.

peptides were constructed by recombining ILBP-a and ILBP-b in different orders and combinations. As shown in Figure 5, the new different types of combinations conferred the new binding peptides with much stronger affinity and selectivity than ILBP-a and ILBP-b. Moreover, the heterozygous binding peptides (ILBP-ab and ILBP-ba) had much better selectivity than the tandem binding peptides (ILBP-aa and ILBP-bb). The following reasons might be used to explain such results. IL-4R carries a large amount of negative charge. The positively charged amino acids in ILBP-a (K77, R81, K84, R85, R88) or ILBP-b (H1, K2, K12) contributed some electrostatic interactions for binding to IL-4R. Due to having more positively charged amino acids, the combined ILBPs were capable of exhibiting higher affinity. In addition, each of the combined ILBPs has two critical binding sites that bind efficiently to IL-4R; thus, the combined ILBP has a significantly higher binding probability to IL-4R than ILBP-a or ILBP-b, resulting in a stronger affinity. Since only one of the R88 residues in ILBP-aa or the E9 residues in ILBP-bb could bind to IL-4R, the patterns of selectivity for ILBP-aa and ILBP-bb remained the same as for ILBP-a and ILBP-b (Figure 4(C)). The heterozygous fusion peptide confers better selectivity to the new binding peptide than the tandem fusion method. In the heterozygous fusion peptides, although ILBP-ab and ILBP-ba differ only in the order of linkage, they exhibited different selectivity (Figure 4(C)). We hypothesise that the positions of several key binding amino acid residues in ILBP-ba are similar to those in native IL-4, hence these residues are able to specifically bind to IL-4R in a more suitable manner than in ILBP-ab. ILBP-ba and IL-4R might form the 'avocado cluster' (residues I5, K12, T13 and N89 of ILBP-ba and Y13, A71, Y183 and Y127 of IL-4R α) to lead the low dielectricity of the microenvironment. The polar interaction of E9 and IL-4R is reinforced by the low dielectricity of the microenvironment, which could greatly enhance the binding of E9 and IL-4R [14]. Therefore, ILBP-ba has a better affinity and selectivity.

Currently, the most commonly used receptors for treating tumours include EGFR [2], HER2 [3] and VEGFR [4]. For EGFR, one of the most prominent peptides targeting peptide GE11 could effectively deliver drugs (lytic peptides, siRNAs and small molecule compounds) into a variety of tumour cells overexpressing EGFR [37–41]. However, according to the report, the IC₅₀ values of the lytic peptide delivered by GE11 were only decreased approximately threefold in tumour cells and 1.3- to 2-fold in normal cells [40]. The fold difference between the two types of cells was not

obvious. Meanwhile, there was no strict positive correlation between fold improvement and EGFR expression levels. However, in our study, ILBP-ba increased the IC₅₀ of TCS more than 10 folds in IL-4R high-expressing cells (A549, H226 and HeLa), and only 1.2 folds in IL-4R low-expressing cells (SMMC). Furthermore, the fold improvements were strictly positively correlated with the IL-4R expression levels in these four cell lines, indicating that ILBP-ba has better specificity and selectivity than GE11 in terms of differential effects.

In conclusion, we constructed a more potent IL-4R-binding peptide, ILBP-ba, which is derived from IL-4 and could specifically deliver drugs into cells overexpressing IL-4R. In addition, this paper also demonstrates that the strategy of designing targeting peptides by containing more high-affinity binding residues of natural ligands to achieve high selectivity is highly effective and provides a new idea for the development of targeting peptides.

Disclosure statement

The authors declare that they have no conflicts of interest regarding the conduct or outcomes of this study.

Funding

This work was supported by the National Natural Science Foundation of China (Grant No. 81571795).

References

- [1] Mathew M, Verma RS. Humanized immunotoxins: a new generation of immunotoxins for targeted cancer therapy. *Cancer Sci*. 2009;100(8):1359–1365.
- [2] Chistiakov DA, Chekhonin IV, Chekhonin VP. The EGFR variant III mutant as a target for immunotherapy of glioblastoma multiforme. *Eur J Pharmacol*. 2017;810:70–82.
- [3] Megan G, Kelly CM, Andrea C. HER2: an emerging target in colorectal cancer. *Curr Probl Cancer*. 2018;42(6):560–571.
- [4] Shibuya M. VEGF-VEGFR system as a target for suppressing inflammation and other diseases. *Endocr Metab Immune Disord Drug Targets*. 2015;15(2):135–144.
- [5] Normanno N, De Luca A, Bianco C, et al. Epidermal growth factor receptor (EGFR) signaling in cancer. *Gene*. 2006;366(1):2–16.
- [6] Chi L, Na MH, Jung HK, et al. Enhanced delivery of liposomes to lung tumor through targeting interleukin-4 receptor on both tumor cells and tumor endothelial cells. *J Control Release*. 2015;209:327–336.
- [7] Zhou C, Wu YL, Chen G, et al. Erlotinib versus chemotherapy as first-line treatment for patients with advanced EGFR mutation-positive non-small-cell lung cancer (OPTIMAL, CTONG-0802): a multicentre, open-label, randomised, phase 3 study. *Lancet Oncol*. 2011;12(8):735–742.
- [8] Rosell R, Carcereny E, Gervais R, et al. Erlotinib versus standard chemotherapy as first-line treatment for European patients with advanced EGFR mutation-positive non-small-cell lung cancer (EURTAC): a multicentre, open-label, randomised phase 3 trial. *Lancet Oncol*. 2012;13(3):239–246.
- [9] Chong CR, Janne PA. The quest to overcome resistance to EGFR-targeted therapies in cancer. *Nat Med*. 2013;19(11):1389–1400.
- [10] Susumu K, Boggon TJ, Tajhal D, et al. EGFR mutation and resistance of non-small-cell lung cancer to gefitinib. *N Engl J Med*. 2005;352(8):786–792.
- [11] Guruprasath P, Kim J, Gunassekaran GR, et al. Interleukin-4 receptor-targeted delivery of Bcl-xL siRNA sensitizes tumors to chemotherapy and inhibits tumor growth. *Biomaterials*. 2017;142:101–111.
- [12] Natoli A, Lupertz R, Merz C, et al. Targeting the IL-4/IL-13 signaling pathway sensitizes Hodgkin lymphoma cells to chemotherapeutic drugs. *Int J Cancer*. 2013;133(8):1945–1954.
- [13] Joshi BH, Leland P, Lababidi S, et al. Interleukin-4 receptor alpha overexpression in human bladder cancer correlates with the pathological grade and stage of the disease. *Cancer Med*. 2014;3(6):1615–1628.
- [14] Mueller TD, Zhang JL, Sebald W, et al. Structure, binding, and antagonists in the IL-4/IL-13 receptor system. *Biochim Biophys Acta*. 2002;1592(3):237–250.
- [15] Kawakami M, Kawakami K, Stepensky VA, et al. Interleukin 4 receptor on human lung cancer: a molecular target for cytotoxin therapy. *Clin Cancer Res*. 2002;8(11):3503–3511.
- [16] Venmar KT, Carter KJ, Hwang DG, et al. IL4 receptor ILR4alpha regulates metastatic colonization by mammary tumors through multiple signaling pathways. *Cancer Res*. 2014;74(16):4329–4340.
- [17] Todaro M, Lombardo Y, Francipane MG, et al. Apoptosis resistance in epithelial tumors is mediated by tumor-cell-derived interleukin-4. *Cell Death Differ*. 2008;15(4):762–772.
- [18] Todaro M, Alea MP, Di Stefano AB, et al. Colon cancer stem cells dictate tumor growth and resist cell death by production of interleukin-4. *Cell Stem Cell*. 2007;1(4):389–402.
- [19] Conticello C, Pedini F, Zeuner A, et al. IL-4 protects tumor cells from anti-cd95 and chemotherapeutic agents via up-regulation of antiapoptotic proteins. *J Immunol*. 2004;172(9):5467–5477.
- [20] Surana R, Wang S, Xu W, et al. IL4 limits the efficacy of tumor-targeted antibody therapy in a murine model. *Cancer Immunol Res*. 2014;2(11):1103–1112.
- [21] Kawakami K, Kawakami M, Puri RK. Overexpressed cell surface interleukin-4 receptor molecules can be successfully targeted for antitumor cytotoxin therapy. *Crit Rev Immunol*. 2001;21(1–3):299–310.
- [22] Rand RW, Kreitman RJ, Patronas N, et al. Intratumoral administration of recombinant circularly permuted interleukin-4-Pseudomonas exotoxin in patients with high-grade glioma. *Clin Cancer Res*. 2000;6(6):2157–2165.
- [23] Koji K, Kawakami M, Husain SR, et al. Targeting interleukin-4 receptors for effective pancreatic cancer therapy. *Cancer Res*. 2002;62(13):3575.
- [24] Weber F, Asher A, Bucholz R, et al. Safety, tolerability, and tumor response of IL4-Pseudomonas exotoxin (NBI-3001) in patients with recurrent malignant glioma. *J Neuro Oncol*. 2003;64(1–2):125–137.
- [25] Garland L, Gitlitz B, Ebbinghaus S, et al. Phase I trial of intravenous IL-4 pseudomonas exotoxin protein (NBI-3001) in patients with advanced solid tumors that express the IL-4 receptor. *J Immunother*. 2005;28(4):376–381.
- [26] Yang L, Horibe T, Kohno M, et al. Targeting interleukin-4 receptor alpha with hybrid peptide for effective cancer therapy. *Mol Cancer Ther*. 2012;11(1):235–243.
- [27] Ishige K, Shoda J, Kawamoto T, et al. Potent in vitro and in vivo antitumor activity of interleukin-4-conjugated

- Pseudomonas* exotoxin against human biliary tract carcinoma. *Int J Cancer*. 2008;123(12):2915–2922.
- [28] Guo C, Ouyang Y, Cai J, et al. High expression of IL-4R enhances proliferation and invasion of hepatocellular carcinoma cells. *Int J Biol Markers*. 2017;32(4):384–390.
- [29] Liu R, Li X, Xiao W, et al. Tumor-targeting peptides from combinatorial libraries. *Adv Drug Deliv Rev*. 2017;110–111:13–37.
- [30] Seto K, Shoda J, Horibe T, et al. Targeting interleukin-4 receptor alpha by hybrid peptide for novel biliary tract cancer therapy. *Int J Hepatol*. 2014;2014:1–7.
- [31] Mei H, Hu Y, Wang H, et al. Binding of EGF1 domain peptide in coagulation factor VII with tissue factor and its implications for the triggering of coagulation. *J Huazhong Univ Sci Technol [Med Sci]*. 2010;30(1):42–47.
- [32] Chen H, Niu X, Gao A, et al. Mitochondrial signal peptide guides EGFP-GRP75 fusion proteins into mitochondria. *Chin J Cell Mol Immunol*. 2016;32(10):1311–1316.
- [33] Cao XW, Yang XZ, Du X, et al. Structure optimization to improve the delivery efficiency and cell selectivity of a tumor-targeting cell-penetrating peptide. *J Drug Target*. 2018;26(9):1–28.
- [34] Shin MC, Min KA, Cheong H, et al. Tandem-multimeric F3-gelonin fusion toxins for enhanced anti-cancer activity for prostate cancer treatment. *Int J Pharm*. 2017;524(1–2):101–110.
- [35] Lee S, Xie J, Chen X. Peptides and peptide hormones for molecular imaging and disease diagnosis. *Chem Rev*. 2010;110(5):3087–3111.
- [36] Lin B, Yang XZ, Cao XW, et al. A novel trichosanthin fusion protein with increased cytotoxicity to tumor cells. *Biotechnol Lett*. 2017;39(1):71–78.
- [37] Song S, Liu D, Peng J, et al. Peptide ligand-mediated liposome distribution and targeting to EGFR expressing tumor in vivo. *Int J Pharm*. 2008;363(1–2):155–161.
- [38] Ren H, Gao C, Zhou L, et al. EGFR-targeted poly (ethylene glycol)-distearoylphosphatidylethanolamine micelle loaded with paclitaxel for laryngeal cancer: preparation, characterization and in vitro evaluation. *Drug Deliv*. 2015;22(6):785–794.
- [39] Fan M, Liang X, Yang D, et al. Epidermal growth factor receptor-targeted peptide conjugated phospholipid micelles for doxorubicin delivery. *J Drug Target*. 2016;24(2):111–119.
- [40] Li Z, Zhao R, Wu X, et al. Identification and characterization of a novel peptide ligand of epidermal growth factor receptor for targeted delivery of therapeutics. *FASEB J*. 2005;19(14):1978–1985.
- [41] Kohno M, Horibe T, Haramoto M, et al. A novel hybrid peptide targeting EGFR-expressing cancers. *Eur J Cancer*. 2011;47(5):773–783.